ELSEVIER

One-dimensional confinement of organic molecules via selective adsorption on CaF$_1$ versus CaF$_2$

H. Rauscher [a,*], T.A. Jung [a,1], J.-L. Lin [a], A. Kirakosian [a], F.J. Himpsel [a], U. Rohr [b], K. Müllen [b]

[a] *Department of Physics, University of Wisconsin–Madison, 1150 University Avenue, Madison, WI 53706-1390, USA*
[b] *Max-Planck-Institut für Polymerforschung, Ackermannweg 10, D-55128 Mainz, Germany*

Abstract

We have integrated one-dimensional organic structures into semiconductor/insulator nanostructures by controlled self-assembly. Stepped Si(111) surfaces with self-organized CaF$_1$/CaF$_2$ stripe patterns serve as mask for selective adsorption of 3,10-di(propyl)perylene. These molecules adsorb preferentially on CaF$_1$ nanostripes, rather than on CaF$_2$. This property is used to fabricate large assemblies of parallel, equidistant stripes 1–15 nm wide. We discuss the selectivity in terms of a mechanism where the HOMO and LUMO of the molecule interact with the valence band and conduction band of CaF$_1$ and CaF$_2$. © 1999 Elsevier Science B.V. All rights reserved.

The ability to fabricate structures with characteristic dimensions of a few nanometers is a key prerequisite for future applications in nanoelectronics [1], nanooptics [2] or as functional materials on the nanometer scale [3,4]. With the reduced size of future molecular devices the effects of dimensionality are becoming more and more important. For example, one-dimensional nanostructures should exhibit unique fundamental physical properties such as density of states singularities or discrete molecular electronic states extending over large linear distances [5]. Technologically useful nanostructures will require lateral dimensions of less than 10 nm so that

the energy separation between quantized electronic states becomes larger than the thermal energy at room temperature. Fabricating such structures still remains a challenge, since one has to be able to combine different materials to fully control their functional properties. Their size needs to be homogeneous within nanometer dimensions and macroscopic quantities of nanostructures need to be produced within a reasonable time. Previous results on the assembly of one-dimensional nanostructures [6–13] have shown that there are rather stringent limits on the speed of fabrication, on the area that can be patterned and on the possible choice of materials.

Here we use the distinct local chemical reactivities of a self-organized CaF$_1$/CaF$_2$ stripe structure on Si(111) to fabricate arrays of one-dimensional organic structures 1–15 nm wide. Thereby, an integrated insulator/semiconductor/soft-matter nanostructure system is assembled from the bottom up

* Corresponding author. Present address: Abteilung Oberflächenchemie und Katalyse, Universität Ulm, 89069 Ulm, Germany. E-mail: hubert.rauscher@chemie.uni-ulm.de
[1] Permanent address: Paul Scherrer Institut, CH-5232 Villingen PSI, Switzerland.

with nanometer precision. All steps are achieved by self-assembly. We first prepare a self-organized step array on a Si(111) surface, coat it with a self-assembled CaF_1/CaF_2 stripe pattern, and finally deposit organic molecules selectively. We show that 3,10-di(propyl)perylene (DPP) molecules exhibit a much higher reactivity towards CaF_1 than towards CaF_2. When these molecules adsorb on the nanometer-wide stripes of CaF_1 they form arrays of self-organized one-dimensional organic structures. We discuss the selective adsorption in terms of a mechanism where the HOMO and LUMO of DPP interacts with the valence and conduction band of CaF_1 and CaF_2.

The fabrication of the compound nanostructures is realized in a three-step process under ultra high vacuum (UHV) conditions. In the first step, a Si(111) surface is conditioned to serve as a template for subsequent building of one-dimensional calcium fluoride nanostructures. Regular step arrays can be produced on Si(111)-(7 × 7) surfaces with periodicities in the 10 nm region [14,15], by a special annealing sequence. Here we used Si(111) with a miscut of 1.1° towards the $[\bar{1}\bar{1}2]$ direction. In this case the annealing procedure yields an atomically clean Si surface with strictly parallel bilayer steps that are aligned along the $[\bar{1}10]$ direction and separated by about 16 nm wide terraces.

In the second step, a mask for molecule deposition is fabricated by deposition of CaF_2 stripes on the regularly stepped Si surface. Calcium fluoride, which is evaporated from a boron nitride crucible, is chosen as mask material because its lattice constant matches that of silicon within 1% and it does not intermix at the silicon interface. After deposition of CaF_2 at 610°C and subsequent annealing to 830°C for 10 s a Si–Ca–F interface is formed where the Ca atoms bond directly to Si [16] and form an interface layer of CaF_1 stoichiometry. If more than a monolayer of CaF_2 is deposited, the Si surface is covered completely by a CaF_1 layer after annealing. CaF_2 in excess of one monolayer is mobile enough during the high-temperature annealing step to diffuse to the steps where it accumulates along the upper step edges and forms continuous stripes [16]. The lateral extension of these stripes can be controlled from about 1 nm to almost a full terrace width of 16 nm by the amount of CaF_2. As a result of this deposition/annealing procedure we obtain a pattern of

alternating CaF_2 and CaF_1 stripes that are several nanometers wide (see the schematic drawing in Fig. 1 and the corresponding scanning tunneling microscope (STM) image in Fig. 2a). It can now serve as a mask for further deposition.

The sequence of preparation steps for the one-dimensional organic nanostructures is illustrated with the STM images in Fig. 2a–c. The STM image on Fig. 2a shows the bare patterned $CaF_2/CaF_1/Si(111)$ surface. For deposition of one-dimensional organic structures on that surface we use 3,10-di(propyl)perylene (right part of Fig. 1). This molecule has a planar structure, and it is expected to interact with a surface via the delocalized electrons of its π electron system. During exposure of the patterned $CaF_2/CaF_1/Si(111)$ surface to DPP at a surface temperature of up to 270°C the molecules adsorb on the entire surface. No preferential bonding of the molecules either to CaF_2 or to CaF_1 is observed, as shown in the STM image of Fig. 2b. The stripe pattern of the $CaF_2/CaF_1/Si(111)$ mask can still be recognized in that image, since molecules adsorbed on CaF_2 appear topographically higher than those on CaF_1. Individual molecules are clearly imaged as discrete protrusions at room temperature, indicating that they are immobile.

The topography changes drastically upon annealing the as-deposited surface to 320°C (Fig. 2c) or by exposure at that temperature. The CaF_1 trenches are still covered with molecules, which again show up as discrete protrusions. The molecules on the CaF_1 regions do not exhibit long-range order. However, after the annealing step the CaF_2 stripes are free of molecules, and their original, pristine topography is regained. The molecules entirely cover the CaF_1
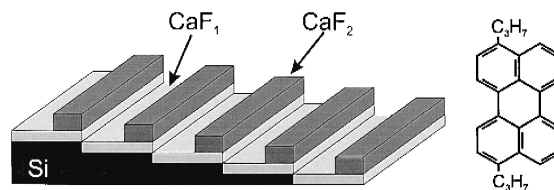
Fig. 1. Left: Schematic model of the Si(111) surface patterned with CaF_2/CaF_1 stripes. The Si(111) surface exhibits straight, regularly spaced steps aligned along the $[\bar{1}10]$ direction. It is completely covered by a monolayer with CaF_1 stoichiometry. CaF_2 stripes are attached to the upper step edges. Right: Model of the 3,10-di(propyl)perylene molecule.
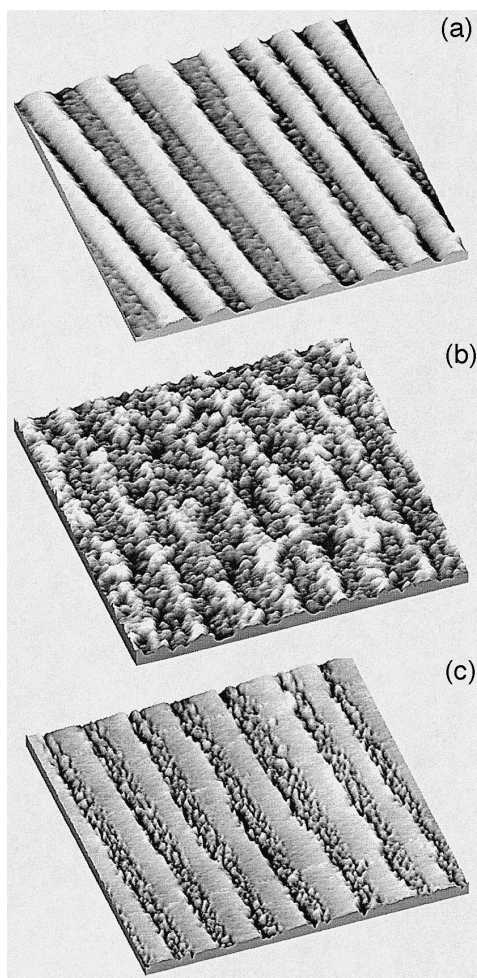
Fig. 2. STM images of the patterned CaF_2 /CaF_1 /Si(111) surface. (a) After growth of the CaF_2 /CaF_1 mask, (b) covered everywhere with DPP at ∼ 270°C, and (c) covered selectively in the CaF_1 trenches after an additional annealing step to ∼ 320°C for 1 min. The CaF_2 stripes and the CaF_1 trenches are each about 8 nm wide. Image sizes: 120 × 120 nm.

CaF_2 stripes and only 4 nm wide CaF_1 trenches. Thus, the molecules can be cast into artificial structures of tailored width by using a CaF_2 mask.

The key for understanding the chemical selectivity of the CaF_2/CaF_1 mask and to predict a possible transferability to other adsorbates lies in the strikingly different electronic structures of the CaF_2 and the CaF_1 films. Earlier investigations [17–20] yielded a comprehensive picture of the CaF_2/CaF/Si(111) interface structure with its Si–Ca–F interface layer which develops during thermal treatment above 700°C. In the CaF_2 layer Ca donates both of its two 4s electrons to the surrounding F atoms. The resulting closed-shell electronic configurations for both Ca and F in CaF_2 give rise to a rather large bandgap of 12 eV, with the conduction band minimum (CBM) about 4 eV above the Fermi energy (E_F). In contrast, the CaF_1 layer has an optical bandgap of only 2.4 eV [21], with the CBM about 2 eV above E_F [19,22]. The local band gap changes by as much as 9.6 eV from the CaF_2 stripes to the CaF_1 trenches. These different band structures allow also to distinguish between CaF_1 and CaF_2 in STM measurements [22]. Chemical imaging of CaF_1 and CaF_2 is possible in this system because there are pronounced resonances at the conduction band minima in the $(d \ln I / d \ln V)$ tunneling spectra.

In DPP, one would expect the HOMO and LUMO (an antibonding π^* orbital [23]) to dominate chemi-

regions, and form a regular array of one-dimensional organic structures, following the given pattern of the calcium fluoride mask. In that example the CaF_2 stripes and CaF_1 trenches are equally wide, about 8 nm. The width of the organic structures can be controlled by the quantity of initially deposited CaF_2. This is evident from the smaller scale image in Fig. 3, where a mask with wider CaF_2 stripes was used. In that example, initially 1.75 monolayers of CaF_2 were deposited. This gives a mask with 12 nm wide

Fig. 3. STM image showing the one-dimensional DPP structures on the patterned Si surface in more detail. The width of the CaF_2 stripes is ∼ 12 nm and that of the CaF_1 trenches ∼ 4 nm. Image size: (60 × 60 nm).
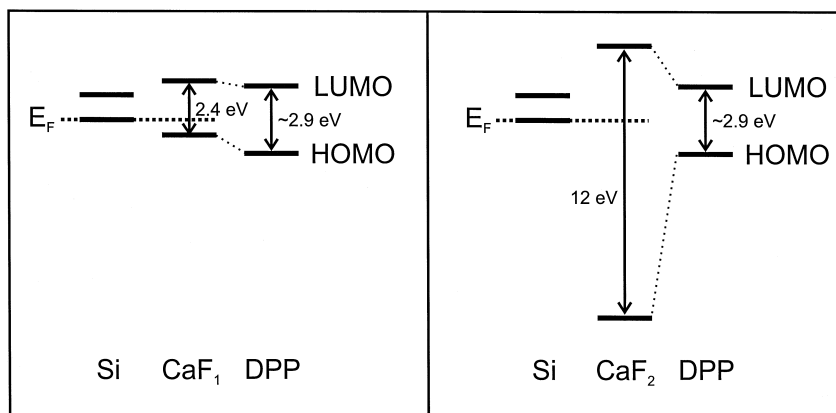
Fig. 4. Schematic line up of the molecular HOMO/LUMO relative to the valence and conduction bands of Si, CaF_1 and CaF_2. The level mismatch for CaF_2 (right) explains the weaker bonding of DPP to CaF_2.

cal bonding of the molecule to the surface. These levels are expected to be similar to those for perylene, which are 2.9 eV apart [24,25]. The energetic position of the DPP orbitals with respect to the CaF_1 and CaF_2 band structures is not known exactly. Therefore we assume here that the Si Fermi level is midway between the HOMO and LUMO of DPP. However, even if the relative position of the Si Fermi level is slightly different, the HOMO–LUMO energy difference of DPP matches the CaF_1 band gap much better than that of CaF_2 (see Fig. 4). CaF_1 should be able to interact more readily with the DPP π electron system. This explains the stronger bonding. For confining the molecules exclusively to the CaF_1 trenches, the weak van der Waals interaction of DPP with CaF_2 needs to be overcome by annealing, such that the molecules diffuse from the CaF_2 stripes to the CaF_1 trenches.

We expect the chemical selectivity observed here to hold for many other adsorbate species. In fact, we already have evidence for selective adsorption of several other molecules on the CaF_2/CaF_1 masked Si surface, including C_{60}, nickelocene, ferrocene and binaphtyl-C3 [26]. By exploiting both the possibility of fabricating masks with nanometer-size features and the chemical selectivity of the $CaF_2/CaF_1/Si(111)$ system a number of exciting applications can be anticipated, including the fabrication of nanocluster strings or even nanometer-wide metallic stripes by selective chemical vapor deposition of organometallic molecules.

In conclusion, we are able to produce parallel, regularly spaced one-dimensional organic structures of adjustable width on patterned Si surfaces. An integrated nanostructure is obtained that contains a semiconductor, an insulator, and organic matter, all put together by self-assembly. An important step is the preferential adsorption of DPP on CaF_1 versus CaF_2. This is explained by a model where the HOMO and LUMO of the molecules interact with the valence band and the conduction band of CaF_1 and CaF_2. In the future, such compound nanostructures may lead to the integration of molecular devices into silicon electronics.

References

[1] F.J. Himpsel, J.E. Ortega, G.J. Mankey, R.F. Willis, Adv. Phys. 47 (1998) 511.
[2] A.P. Alivisatos, Science 271 (1996) 933.
[3] M. Sundaram, S.A. Chalmers, P.F. Hopkins, A.C. Gossard, Science 254 (1991) 1326.
[4] G.M. Whitesides, J.P. Matthias, C.T. Seto, Science 254 (1991) 1312.
[5] C.M. Lieber, Solid State Commun. 107 (1998) 607.
[6] J.W. Lyding, T.-C. Shen, J.S. Hubacek, J.R. Tucker, G.C. Abeln, Appl. Phys. Lett. 64 (1994) 2010.

[7] T.-C. Shen, C. Wang, G.C. Abeln, J.R. Tucker, J.W. Lyding, Ph. Avouris, R.E. Walkup, Science 268 (1995) 1590.

[8] E.T. Foley, A.F. Kam, J.W. Lyding, Ph. Avouris, Phys. Rev. Lett. 80 (1998) 1336.

[9] M.F. Crommie, C.P. Lutz, D.M. Eigler, Science 262 (1993) 218.

[10] P.W. Murray, I.M. Brookes, S.A. Haycock, G. Thornton, Phys. Rev. Lett. 80 (1998) 988.

[11] R.M. Silver, E.E. Ehrichs, A.L. de Lozanne, Appl. Phys. Lett. 51 (1987) 247.

[12] H. Rauscher, F. Behrendt, R.J. Behm, J. Vac. Sci. Technol. B 15 (1997) 1373.

[13] F.J. Himpsel, T.A. Jung, J.E. Ortega, Surf. Ref. Lett. 4 (1997) 371.

[14] J. Viernow, J.-L. Lin, D.Y. Petrovykh, F.M. Leibsle, F.K. Men, F.J. Himpsel, Appl. Phys. Lett. 72 (1998) 948.

[15] J.-L. Lin, D.Y. Petrovykh, J. Viernow, F.K. Men, D.J. Seo, F.J. Himpsel, J. Appl. Phys. 84 (1998) 255.

[16] D.Y. Petrovykh, J. Viernow, J.-L. Lin, F.M. Leibsle, F.K. Men, A. Kirakosian, F.J. Himpsel, submitted to J. Vac. Sci. Technol.; J. Viernow, D.Y. Petrovykh, F.K. Men, A. Kirakosian, J.-L. Lin, F.J. Himpsel, Appl. Phys. Lett., in press.

[17] R.M. Tromp, M.C. Reuter, Phys. Rev. Lett. 61 (1988) 1756.

[18] M.A. Olmstead, R.I.G. Uhrberg, R.D. Bringans, R.Z. Bachrach, Phys. Rev. B 35 (1987) 7526.

[19] D. Rieger, F.J. Himpsel, U.O. Karlsson, F.R. McFeely, J.F. Morar, J.A. Yarmoff, Phys. Rev. B 34 (1986) 7295.

[20] J. Zegenhagen, J.R. Patel, Phys. Rev. B 41 (1990) 5315.

[21] T.F. Heinz, F.J. Himpsel, E. Palange, E. Burstein, Phys. Rev. Lett. 63 (1989) 644.

[22] J. Viernow, D.Y. Petrovykh, A. Kirakosian, J.-L. Lin, F.K. Men, M. Henzler, F.J. Himpsel, Phys. Rev. B, in press.

[23] J. Schiedt, R. Weinkauf, Chem. Phys. Lett. 274 (1997) 18.

[24] C. Bouzou, C. Jouvet, J.B. Leblond, Ph. Millie, A. Tramer, M. Sulkes, Chem. Phys. Lett. 97 (1983) 161.

[25] S. Grimme, H.-G. Löhmannsröben, J. Phys. Chem. 96 (1992) 7005.

[26] H. Rauscher, T.A. Jung, J.-L. Lin, A. Kirakosian, J.J. Himpsel, unpublished.